VOLUME 30 NUMBER 4 October 2024
pISSN 2287-2728
eISSN 2387-285X

CLINICAL and MOLECULAR HEPATOLOGY

The forum for latest knowledge of hepatobiliary diseases

T-cell therapy for HBV-HCC

Mortality from HCC and biliary tract cancers
Liver fibrosis scores and viral load in CHB
Genomic biomarkers for atezolizumab+bevacizumab in HCC
Epigenetic alteration of complement genes in MASLD

KASL

pISSN 2287-2728
eISSN 2287-285X

CLINICAL and MOLECULAR HEPATOLOGY

https://doi.org/10.3350/cmh.2024.0229
Clinical and Molecular Hepatology 2024;30:824-844

Original Article

DNA methylome analysis reveals epigenetic alteration of complement genes in advanced metabolic dysfunction-associated steatotic liver disease

Amal Magdy[1,2,*], Hee-Jin Kim[1,*], Hanyong Go[1,2], Jun Min Lee[1,2], Hyun Ahm Sohn[1], Keeok Haam[1], Hyo-Jung Jung[1], Jong-Lyul Park[1,2], Taekyeong Yoo[3], Eun-Soo Kwon[1,4], Dong Hyeon Lee[5], Murim Choi[3], Keon Wook Kang[6], Won Kim[5], and Mirang Kim[1,2] on behalf of the Innovative Target Exploration of NAFLD (ITEN) Consortium

[1]Aging Convergence Research Center, Korea Research Institute of Bioscience and Biotechnology (KRIBB), Daejeon; [2]Department of Functional Genomics, KRIBB School of Bioscience, Korea University of Science and Technology (UST), Daejeon; [3]Department of Biomedical Sciences, Seoul National University College of Medicine, Seoul; [4]Department of Biomolecular Science, KRIBB School of Bioscience, UST, Daejeon; [5]Department of Internal Medicine, Seoul National University College of Medicine, Seoul Metropolitan Government Boramae Medical Center, Seoul; [6]College of Pharmacy and Research Institute of Pharmaceutical Sciences, Seoul National University, Seoul, Korea

Graphical Abstract

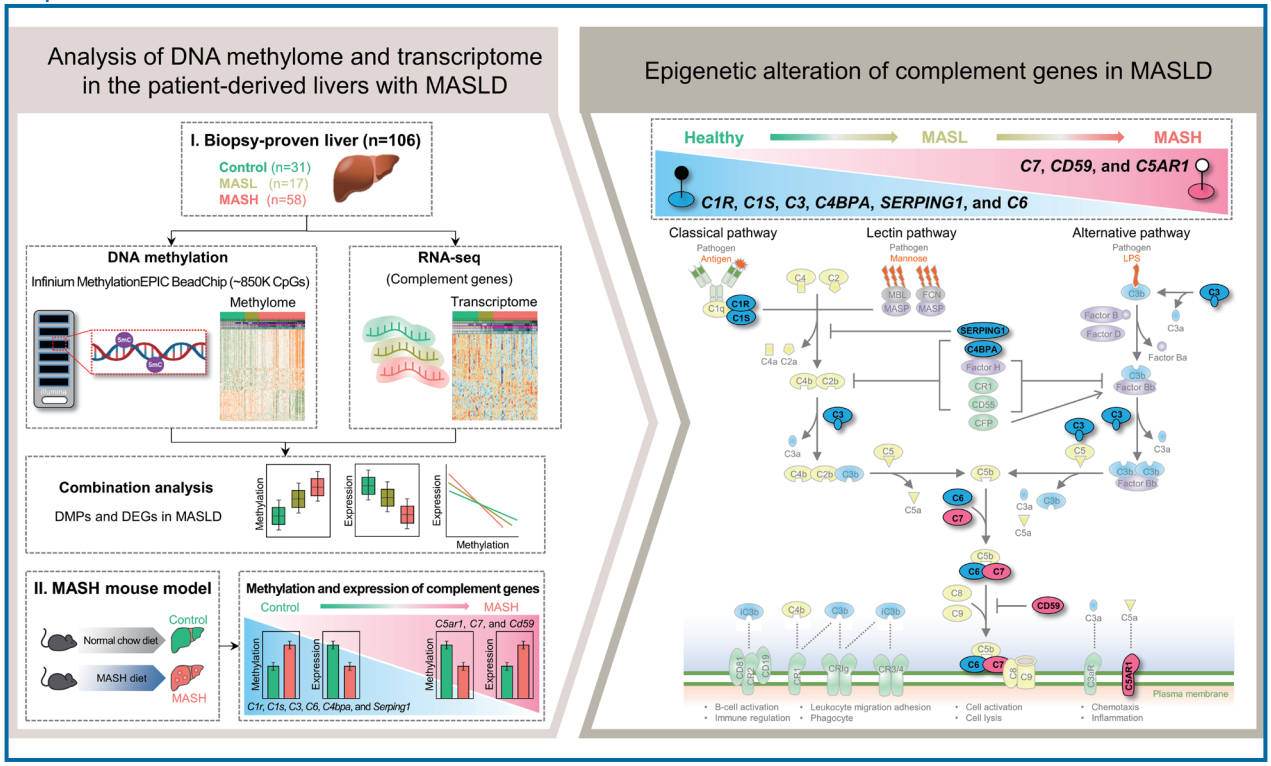

Study Highlights

- Our study provides convincing evidence of epigenetic alteration of complement genes linked to MASLD, as evidenced by hypermethylation and downregulation of the complement genes *C1R*, *C1S*, *C3*, *C6*, *C4BPA*, and *SERPING1* alongside hypomethylation and upregulation of *C5AR1*, *C7*, and *CD59*. These findings offer crucial insights into the mechanisms propelling MASLD progression and suggest that precision-targeted therapies, including the use of inhibitors of the complement system, could be promising strategies for managing MASLD.

Background/Aims: Blocking the complement system is a promising strategy to impede the progression of metabolic dysfunction–associated steatotic liver disease (MASLD). However, the interplay between complement and MASLD remains to be elucidated. This comprehensive approach aimed to investigate the potential association between complement dysregulation and the histological severity of MASLD.

Methods: Liver biopsy specimens were procured from a cohort comprising 106 Korean individuals, which included 31 controls, 17 with isolated steatosis, and 58 with metabolic dysfunction–associated steatohepatitis (MASH). Utilizing the Infinium Methylation EPIC array, thorough analysis of methylation alterations in 61 complement genes was conducted. The expression and methylation of nine complement genes in a murine MASH model were examined using quantitative RT-PCR and pyrosequencing.

Results: Methylome and transcriptome analyses of liver biopsies revealed significant (P<0.05) hypermethylation and downregulation of *C1R*, *C1S*, *C3*, *C6*, *C4BPA*, and *SERPING1*, as well as hypomethylation (P<0.0005) and upregulation (P<0.05) of *C5AR1*, *C7*, and *CD59*, in association with the histological severity of MASLD. Furthermore, DNA methylation and the relative expression of nine complement genes in a MASH diet mouse model aligned with human data.

Conclusions: Our research provides compelling evidence that epigenetic alterations in complement genes correlate with MASLD severity, offering valuable insights into the mechanisms driving MASLD progression, and suggests that inhibiting the function of certain complement proteins may be a promising strategy for managing MASLD. **(Clin Mol Hepatol 2024;30:824-844)**

Keywords: MASLD; MASH; DNA methylation; Complement; Epigenetics

INTRODUCTION

Metabolic dysfunction-associated steatotic liver disease (MASLD), formerly known as nonalcoholic fatty liver disease (NAFLD), has undergone a redefinition to encompass liver steatosis accompanied by cardiometabolic risk factors.[1] This spectrum of histopathological findings includes metabolic dysfunction-associated steatotic liver (MASL; isolated steatosis) and metabolic dysfunction–associated steatohepatitis (MASH), previously referred to as nonalcoholic steatohepatitis (NASH). MASH represents the inflammatory subtype of MASLD, carrying a significant risk for progression to cirrhosis and hepatocellular carcinoma (HCC). Individuals diagnosed with MASH face an elevated

Corresponding author : Mirang Kim
Aging Convergence Research Center, Korea Research Institute of Bioscience and Biotechnology (KRIBB),125 Gwahak-ro, Yuseong-gu, Daejeon 34141, Korea
Tel: +82-42-879-8113, Fax: +82-42-879-8119, E-mail: mirang@kribb.re.kr
https://orcid.org/0000-0001-7415-0077

Won Kim
Department of Internal Medicine, Seoul National University College of Medicine, Seoul Metropolitan Government Boramae Medical Center, Boramae-ro 5-gil, Dongjak-gu, Seoul 07061, Korea
Tel: +82-2-870-2233, Fax: +82-2-831-2826, E-mail: drwon1@snu.ac.kr
https://orcid.org/0000-0002-2926-1007

*These authors contributed equally as first authors.

Editor: Silvia Sookoian, CONICET (National Scientific and Technical Research Council), Argentina **Received :** Apr. 9, 2024 / **Revised :** Jul. 22, 2024 / **Accepted :** Jul. 24, 2024

Abbreviations:

MASLD, metabolic dysfunction-associated steatotic liver disease; NAFLD, nonalcoholic fatty liver disease; MASL, metabolic dysfunction-associated steatotic liver; MASH, metabolic dysfunction–associated steatohepatitis; NASH, nonalcoholic steatohepatitis; HCC, hepatocellular carcinoma; NAS, NAFLD activity score; snRNA-seq, single-nucleus RNA-seq; GEO, Gene Expression Omnibus

mortality risk, primarily due to cardiovascular causes. The prevalence of MASLD has surged alongside the worldwide obesity epidemic. Presently, MASLD afflicts approximately 25–30% of adults worldwide, although projections from hierarchical Bayesian analysis suggest that more than half of all adults could be affected by 2040.[2]

The progression of MASLD is influenced by various factors, including diet, lifestyle choices, and composition of the gut microbiome, which collectively can trigger aberrant epigenetic modifications that contribute to disease progression.[3] DNA methylation stands out as a relatively stable epigenetic mechanism governing gene expression patterns. Typically, hypermethylation of DNA can silence gene expression, whereas hypomethylation can activate gene expression. Therefore, investigating the DNA methylome is crucial for identifying biomarkers linked to disease progression as well as for screening potential therapeutic targets. Studies conducted with human liver specimens have revealed associations between MASLD and abnormal patterns of DNA methylation.[4,5] Nevertheless, the epigenetic mechanisms of MASLD are not completely understood.

The complement system is a crucial component of innate immunity that plays a pivotal role in defending against invading pathogens.[6] Complement is comprised of approximately 60 soluble and membrane-bound proteins including core components as well as receptors and regulatory factors.[6] Recent comprehensive assessments of complement function have revealed its multifaceted involvement beyond canonical immune processes. Indeed, complement contributes to essential physiological processes such as resolution of inflammation, clearance of apoptotic cells, angiogenesis, wound healing, stem-cell recruitment and activation, and tissue repair.[7-9] However, age-related processes and deficiencies as well as genetic variations in complement proteins can perturb complement function, with detrimental consequences.[9] Moreover, burgeoning research indicates a significant involvement of the complement system in MASLD progression.[10-12] Despite this pathophysiological connection, our understanding of the interplay between complement and MASLD remains rudimentary, primarily owing to isolated studies that often have been conducted with animal models or *in vitro*.[13] These investigations have yielded varied and occasionally conflicting conclusions,[14] perhaps owing to the complexity of complement's roles in numerous physiological processes. Moreover, the cellular levels of complement components can dictate whether the effects are pro-inflammatory or anti-inflammatory depending on MASLD status.[15]

Analyses of human MASLD cases are scarce, leaving unanswered questions regarding the abundance of complement components in both health and disease and the extent to which they become activated or suppressed in MASLD patients. Debates persist concerning whether complement activation is heightened or suppressed in MASLD and whether the levels of complement components correlate with MASLD severity. To address this issue, we conducted a comprehensive analysis by combining data obtained from DNA methylome and transcriptome studies with the goal of deepening our understanding of the potential link between complement dysregulation and the risk or severity of MASLD.

MATERIALS AND METHODS

Patients

Patients with biopsy-proven MASLD were enrolled following the procedures outlined in our previous study.[16] Approval for this study was obtained from the institutional review board of Seoul Metropolitan Government Boramae Medical Center. We established a prospective cohort from the ongoing Boramae MASLD registry (NCT 02206841) as described previously.[17] The MASLD cohort (ITEN) comprised 106 Korean individuals aged 25–80 who sought medical attention at Seoul Metropolitan Government Boramae Medical Center. Prior to participation, all individuals were fully informed about the study protocol and provided written informed consent.

NAFLD activity score (NAS) and fibrosis stage are assessed according to the Kleiner classification and all study participants were categorized into the control, MASL, and MASH groups (Table 1).[18]

SAF score encompasses three main components: steatosis (S), activity (A), and fibrosis (F). Steatosis is graded from S0 to S3 based on the percentage of the hepatocytes affected by large- or medium-sized lipid droplets. Activity is assessed by the presence and severity of hepatocyte ballooning and lobular inflammation, graded from A0 to A3. Fibrosis is categorized into stages ranging from F0 (no fibro-

https://doi.org/10.3350/cmh.2024.0229

Table 1. Clinical and histological characteristics of study participants

Characteristic	Total (n=106)	Control (n=31)	MASL (n=17)	MASH (n=58)	*P*-value[a]
Male sex	49 (46.2%)	16 (51.6%)	11 (64.7%)	22 (37.9%)	0.116
Continuous variables					
Age (years)	56.0 (44.0, 65.0)	58.0 (48.5, 66.5)	42.0 (35.0, 62.0)	57.5 (45.0, 65.0)	0.130
Body weight (kg)	66.6 (59.4, 78.4)	60.1 (52.9, 66.0)	71.0 (65.4, 82.3)	71.0 (62.1, 81.5)	<0.001
BMI (kg/m^2)	25.6 (23.4, 28.6)	22.9 (21.1, 23.9)	26.5 (24.3, 29.4)	27.2 (25.4, 31.0)	<0.001
ALT (U/L)	42.0 (25.3, 75.5)	22.0 (16.0, 28.5)	36.0 (26.0, 61.0)	63.0 (41.5, 103.5)	<0.001
AST (U/L)	40.0 (24.0, 53.0)	23.0 (20.0, 30.0)	35.0 (23.0, 49.0)	49.5 (40.0, 79.0)	<0.001
HDL cholesterol (mg/dL)	44.5 (37.0, 52.0)	46.0 (38.5, 55.5)	44.0 (40.0, 48.0)	44.5 (34.3, 51.8)	0.755
Total cholesterol (mg/dL)	171.0 (146.5, 200.5)	163.0 (133.0, 192.5)	180.0 (152.0, 196.0)	178.5 (152.0, 203.0)	0.268
TG (mg/dL)	125.0 (89.3, 176.0)	89.0 (81.5, 136.0)	111.0 (90.0, 167.0)	148.5 (110.3, 187.8)	0.001
Albumin (g/dL)	4.1 (3.9, 4.3)	4.0 (3.7, 4.2)	4.3 (4.1, 4.4)	4.1 (3.9, 4.3)	0.015
Concomitant medications					
Antidiabetics	31 (29.2%)	5 (16.1%)	3 (17.6%)	23 (39.7%)	0.035
Antihypertensive drugs	41 (38.7%)	9 (29.0%)	5 (29.4%)	27 (46.6%)	0.188
Statins	34 (32.1%)	12 (38.7%)	6 (35.3%)	16 (27.6%)	0.537
Comorbidities[b]					
Obesity[c]	56 (52.8%)	3 (9.7%)	9 (52.9%)	44 (75.9%)	<0.001
Diabetes	31 (29.2%)	5 (16.1%)	3 (17.6%)	23 (39.7%)	0.035
CVD	12 (11.3%)	3 (9.7%)	1 (5.9%)	8 (13.8%)	0.626
Hypertension	44 (41.5%)	9 (29.0%)	6 (35.3%)	29 (50.0%)	0.137
Dyslipidemia	34 (32.1%)	12 (38.7%)	6 (35.3%)	16 (27.6%)	0.537
Hypothyroidism	10 (9.4%)	4 (12.9%)	0	6 (10.3%)	0.300
Histological features					
Steatosis					
Grade 0 (<5%)	31 (29.2%)	31 (100.0%)	0	0	<0.001
Grade 1 (5–33%)	13 (12.3%)	0	6 (35.3%)	7 (12.1%)	
Grade 2 (33–66%)	19 (17.9%)	0	5 (29.4%)	14 (24.1%)	
Grade 3 (>66%)	43 (40.6%)	0	6 (35.3%)	37 (63.8%)	
Lobular inflammation					
Grade 0	28 (26.4%)	21 (67.7%)	6 (35.3%)	1 (1.7%)	<0.001
Grade 1	53 (50.0%)	10 (32.3%)	10 (58.8%)	33 (56.9%)	
Grade 2	24 (22.6%)	0	1 (5.9%)	23 (39.7%)	
Grade 3	1 (0.9%)	0	0	1 (1.7%)	
Ballooning					
Grade 0	39 (36.8%)	28 (90.3%)	10 (58.8%)	1 (1.7%)	<0.001
Grade 1	62 (58.5%)	3 (9.7%)	7 (41.2%)	52 (89.7%)	
Grade 2	5 (4.7%)	0	0	5 (8.6%)	
Fibrosis stage					
F0	30 (28.3%)	26 (83.9%)	4 (23.5%)	0	<0.001
F1	37 (34.9%)	4 (12.9%)	11 (64.7%)	22 (37.9%)	
F2	26 (24.5%)	1 (3.2%)	2 (11.8%)	23 (39.7%)	
F3	3 (2.8%)	0	0	3 (5.2%)	
F4	10 (9.4%)	0	0	10 (17.2%)	

MASL, metabolic dysfunction-associated steatotic liver; MASH, metabolic dysfunction-associated steatohepatitis; CVD, cardiovascular disease; BMI, body mass index; ALT, alanine aminotransferase; AST, aspartate aminotransferase; HDL, high-density lipoprotein; TG, triglycerides.

[a]Categorical data are expressed as the number (%), and the differences between groups were determined by the χ^2 test. Continuous variables are expressed as the median (interquartile range), and differences between groups were determined by the Kruskal–Wallis test.

[b]The presence of these comorbidities is based on a combination of medical history and medication use in their medical records. For example, if someone was taking statins, then dyslipidemia was identified, etc.

[c]BMI >25.

sis) to F4 (cirrhosis) based on the extent and pattern of fibrosis within the liver tissue. SAF severity was categorized into of '0' (no MASLD; control), '1', '2', and '3' based on the criteria established by Bedossa et al.[19] SAF scoring in our analysis aligns with established severity levels: SAF severity '1' denotes mild severity, characterized by A <2 and F <2. SAF severity '2' indicates significant severity with A ≥2 and/or F ≥2. Finally, SAF severity '3' signifies severe severity, indicating A ≥3 and/or F ≥3.

Liver tissues were collected from healthy control subjects who underwent liver biopsy in a pre-evaluation for becoming a liver transplantation donor, and normal liver parenchyma was collected from patients with intrahepatic benign tumors. In subsequent analyses, we considered the absence of MASLD as a control and either MASL or MASH as the MASLD group.

DNA methylation microarray experiment and data analysis

The EPIC BeadChip (Illumina) was employed for methylation array analyses. Initially, 1 μg genomic DNA sourced from human liver tissue underwent treatment with 20 μL sodium bisulfite solution provided in the EZ DNA Methylation-Gold kit (Zymo Research, Orange, CA, USA). Subsequently, bisulfite-converted DNA (4 μL) was subjected to amplification using the Infinium Methylation Assay kit (Illumina). The amplified DNA was then hybridized onto an EPIC BeadChip and scanned utilizing the Illumina iSCAN system.

To assess the extent of CpG methylation, we utilized the SeSAMe package (v1.20.0) within the R software (v4.3.1), incorporating functional normalization to mitigate technical variabilities. Preliminary processing encompassed several steps: 'qualityMask', 'infniumIChannel', 'dyeBiasNL', 'pOOBAH', and 'noob', aimed at filtering out poor-quality probe data, correcting for dye bias and channel switching, and executing background subtraction. Specifically, CpG probes failing in 10% or more samples, non-CpG probes, probes targeting chromosome X or Y and flagged probes were excluded from the analysis. Additionally, measurements with detection *P*-values of <0.05 were deemed to exhibit a significant signal above background. For publicly available data from GEO (GSE180474),[4] idat files underwent similar preprocessing procedures. Finally, all primary methylation array data were deposited in K-BDS (Korea BioData Station, https://kbds.re.kr) under accession number KAP240571.

RNA-seq data analysis

The RNA sequencing (RNA-seq) data from our previous study encompassed 92 liver samples from 28 control, 16 MASL, and 48 MASH subjects.[16] Total RNA extracted from each liver sample was utilized for RNA sequencing with the HiSeq2500 platform. The reads were subsequently mapped and quantified using the human genome (hg19/GRCh37) reference based on GENCODE v19. Additionally, publicly available data were sourced from GEO (GSE135251).[20] The counts matrix underwent normalization for trimmed mean of M values (i.e., TMM) using the edgeR package (version 4.0.11), followed by conversion to counts per million and subsequent $\log_2$ transformation to yield normalized values. From this normalized matrix, the expression values of complement genes were extracted. Subsequently, we utilized clinical data pertaining to NAS and fibrosis stage to explore the expression patterns of complement genes across various MASLD spectra, employing boxplots for visualization.

Analysis of single-nucleus RNA-seq data

We utilized pre-processed and annotated single-nucleus RNA-seq (snRNA-seq) data from the Gene Expression Omnibus (GEO) under accession number GSE202379.[21] This dataset comprises transcriptomic profiles from 47 liver biopsies representing the entire spectrum of MASLD progression. The snRNA-seq data were merged and annotated into a comprehensive Seurat object (GSE202379_SeuratObject_AllCells.rds) for downstream analysis. We utilized the Seurat package (v4.1.3) for our analysis.

Hepatocytes zonation signature analysis

We employed previously established human zonation marker genes to distinguish portal- and central-zone hepatocytes within healthy and three other conditions.[21-24] The zonation analysis method employed in this study followed the approach outlined in Guilliams et al.[25] For human hepatocytes, this approach successfully identified zonated ex-

https://doi.org/10.3350/cmh.2024.0229

pression patterns of landmark genes, such as *HAL, SDS, ASS1* and *PCK1* (periportal zone) and *CYP2E1, SLCO1B3* and *GLUL* (pericentral zone).[22,23]

Mice

C57BL/6N male mice, 6 weeks old, were purchased from ORIENTBIO (Korea). The mice used in this study were maintained at the Korea Research Institute of Bioscience and Biotechnology in accordance with the guidelines provided by the Institutional Animal Care and Use Committee. Mice were housed in a specific-pathogen-free environment at 23°C, humidity 40–50%, and a 12-h light-dark cycle. Throughout the study, the mice had ad libitum access to water. At age 8 weeks, the experimental mice were divided into two groups. One group was fed a MASH diet (#TD.190142, Teklad Custom Diet; ENVIGO, Indianapolis, IN, USA) supplemented with a sucrose solution (D-glucose=18.9 g/L, fructose=23.1 g/L), whereas the control group was fed a normal chow diet (#2018S, Teklad Global 18% Protein Rodent Diet, ENVIGO). After 14 weeks on the respective diets, the mice were sacrificed and their livers analyzed.

Data analysis and representation

The statistical significance of differences between groups was evaluated using the Kruskal-Wallis test for continuous variables and the chi-square test for categorical variables. The gene expression and DNA methylation heatmap was created using the Heatmap function of the ComplexHeatmap package (version 2.18.0). Boxplots depicting complement genes were generated using the ggplot2 package (version 3.5.0). All statistical analyses were performed in R (version 4.3.2). Findings with a *P*-value <0.05 were deemed statistically significant.

RESULTS

Aberrant methylation and expression of complement genes in MASLD

For the DNA methylome analysis, liver biopsy specimens were collected from 106 Korean individuals with diverse metabolic status and histological status. Employing standardized pathological scores, the samples were categorized into the control (n=31) and MASLD (n=75, comprising 17 MASL and 58 MASH individuals) groups (Fig. 1A and Table 1). To identify DMPs specific for MASLD, we performed a comprehensive genome-wide methylation analysis using the Infinium Methylation EPIC array. We established two criteria for DMP identification: (1) $P<0.005$, and (2) methylation differences greater than 0.05 or less than −0.05 (based on mean β values) between control and MASLD samples. This approach led to the identification of 277,484 DMPs among the MASLD specimens, comprising 106,116 hypermethylated and 171,368 hypomethylated CpGs. The results are illustrated in Supplementary Figure 1 with a Manhattan plot and a quantile-quantile plot.

The complement system can be activated through three separate pathways: the classical pathway, lectin pathway, and alternative pathway (Fig. 1A). These pathways are initiated by pathogen- or damage-associated molecular patterns, each distinguished by specific contextual cues.[6] The HUGO Gene Nomenclature Committee report for the complement system comprises 56 genes, including 27 activation components and 29 regulators and receptors.[6] Additionally, we included 5 genes (*C1RL*, *C1QTNF3*, *C1QTNF9*, *C1QTNF9B*, and *C5AR2*) in the complement gene list (Supplementary Table 1).

To investigate the potential association between the dysregulation of complement genes and MASLD severity, we analyzed DMPs linked to 61 complement genes. This led to the identification of 277 DMPs that were associated with complement genes. Specifically, 187 CpGs were hypermethylated and 90 were hypomethylated in patients with MASLD (Supplementary Table 2). Among the 61 complement genes, 47 had DMPs; 16 had only hypermethylated DMPs, and 7 had only hypomethylated DMPs. The remaining 24 genes had both hypermethylated and hypomethylated DMPs. The supervised hierarchical clustering of the DNA methylation patterns of these DMPs is presented in Figure 1B.

Our analysis involved stratifying samples based on disease severity, specifically focusing on fibrosis (from 0 to 4), lobular inflammation (from 0 to 2), steatosis (from 0 to 3), and NAS (from 0 to 7). Remarkably, we observed concurrent escalation in methylation alterations corresponding to disease severity (Fig. 1B).

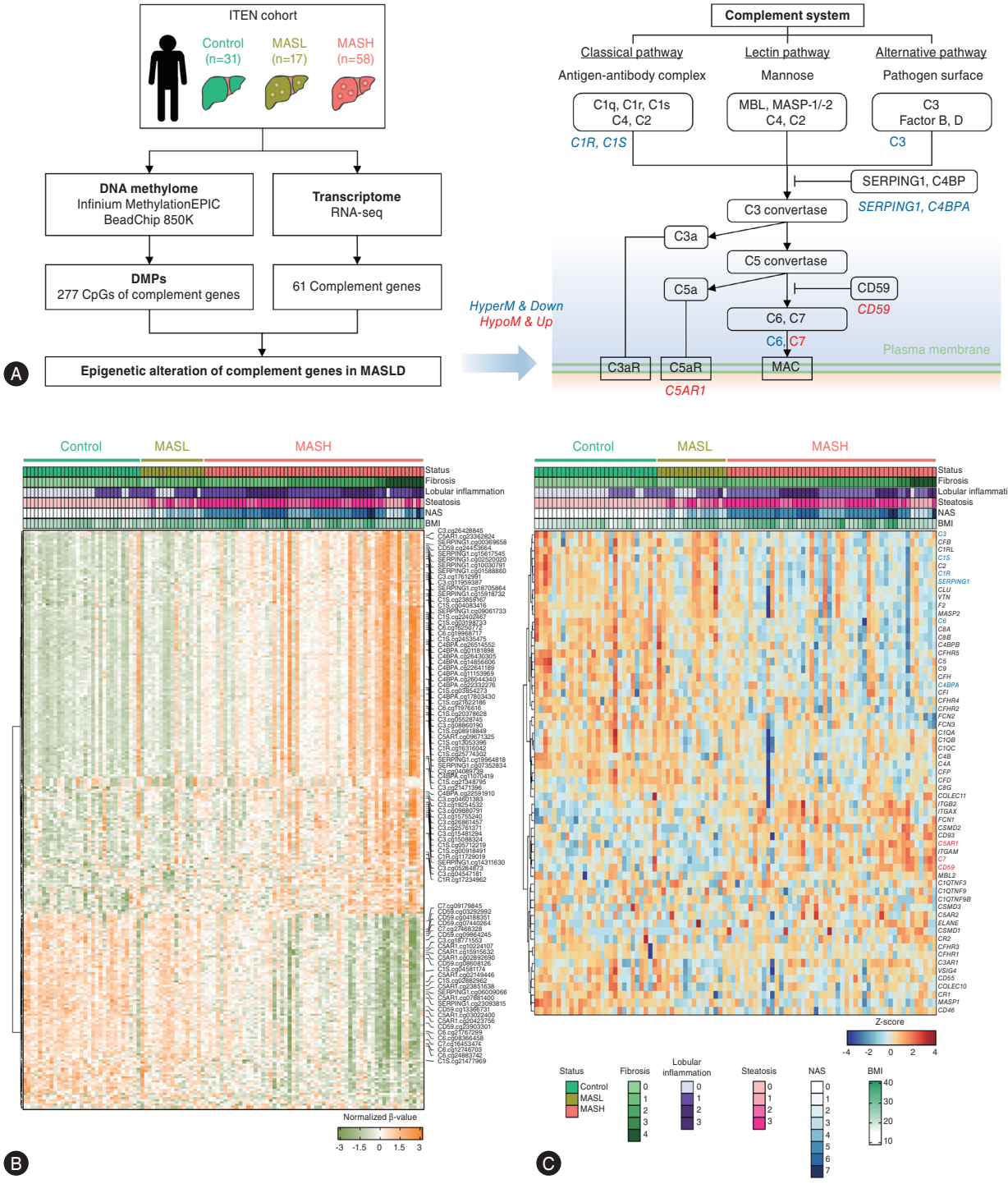

Figure 1. Altered methylation and expression of complement genes in MASLD progression. (A) Left: Schematic of the study design. MASL, metabolic dysfunction-associated steatotic liver; MASH, metabolic dysfunction-associated steatohepatitis; DMPs, differentially methylated CpG positions. Right: Simplified scheme of the complement system. Complement system activation comprises three proteolytic cascades called the classical, lectin, and alternative pathways, all converging at the activation of C3 convertase, a central point in complement activation. This cascade leads to the activation of crucial effectors such as the membrane attack complex (MAC) and anaphylatoxins (C3a and C5a). (B) Heatmap for DNA methylation of complement genes showing changes at CpG sites associated with MASLD progression in the ITEN cohort (106 samples). (C) Heatmap for mRNAs transcribed from complement genes showing changes related to MASLD progression in the ITEN cohort (92 samples).

https://doi.org/10.3350/cmh.2024.0229

Next, we examined the expression of the 61 complement genes utilizing RNA-seq data obtained from 92 specimens (comprising 28 control, 16 MASL, and 48 MASH) included in our previous study[16] (see Fig. 1C for supervised hierarchical clustering of complement gene expression patterns). The expression of complement activation genes, including *C2, C3, C5, C6, C9, C1R,* and *C1S*, declined progressively as disease progressed, whereas the expression of complement regulators and receptors such as *CD59*, *CD93*, and *C5AR1* gradually increased. These findings implied that alterations in DNA methylation patterns of complement genes accumulate with increasing MASLD severity, and these alterations likely impact gene expression.

Defining DMPs associated with complement gene expression

To further elucidate the relationship between DMP methylation and complement gene expression, we conducted a Pearson correlation analysis (Fig. 2A). Among the 277 DMPs examined, 143 CpGs exhibited an inverse correlation (R <–0.3) with complement gene expression, whereas 35 CpGs exhibited a positive correlation (R >0.3). Analysis using ChromHMM state annotation files[26] revealed that DMPs exhibiting an inverse correlation were predominantly located within active promoter regions and strong enhancers in human hepatocytes (Fig. 2B). In contrast, DMPs exhibiting a positive correlation were associated with heterochromatin regions and displayed weaker transcriptional activity (Fig. 2B). These findings implied that, throughout the progression to MASLD, changes in CpG methylation within promoter and enhancer regions of complement genes play a role in modulating gene expression.

Notably, the inverse relationship between complement gene expression and DNA methylation was more evident in MASH samples than in controls. This correlation identified nine genes with an R value less than –0.5 in MASH (Fig. 2C). Within this cohort, *C1R*, *C1S*, *C3*, *C6*, *C4BPA*, and *SERPING1* were downregulated, whereas *C5AR1*, *C7*, and *CD59* were upregulated in MASH (Fig. 1C). Supplementary Figure 2 presents the DMPs associated with MASH in the nine genes. Hypermethylation was observed in DMPs associated with the genes *C1R* (3 DMPs), *C1S* (16 DMPs), *C3* (16 DMPs), *C6* (3 DMPs), *C4BPA* (11 DMPs), and *SERPING1* (11 DMPs), and hypomethylation was observed in DMPs associated with *C5AR1* (8 DMPs), *C7* (3 DMPs), and *CD59* (8 DMPs).

Particularly, the methylation status of *C1R* showed a robust inverse correlation with its expression in MASH (R=–0.58) and MASL (R=–0.47), whereas no discernible correlation was observed in control samples (R=0.013). Similarly, for *C5AR1*, a strong inverse correlation was found in MASH (R=–0.67), with relatively weaker correlations in MASL (R=–0.22) and controls (R=–0.15) (Fig. 2C). These findings suggested that DNA methylation changes within nine complement genes increase with increasing severity of MASLD, with consequent effects on expression.

Methylation patterns of selected complement genes correlate with histological severity of MASLD

We next examined the methylation patterns of nine selected complement genes in correlation with the histological severity of MASLD, encompassing liver fibrosis and NAS. For MASH, there was increased methylation of six genes (*C1R*, *C1S*, *C3*, *C6*, *C4BPA*, and *SERPING1*) alongside decreased methylation of three genes (*C5AR1*, *C7*, and *CD59*) (Fig. 3A). The methylation patterns of the nine genes in MASLD were consistent with liver steatosis (Supplementary Fig. 3), lobular inflammation (Supplementary Fig. 4), and ballooning (Supplementary Fig. 5).

Furthermore, our analysis extended to assessing methylation levels across various liver fibrosis stages, ranging from 0 to 4. Notably, significant disparities in complement gene methylation emerged between the most advanced stages (F3–4) and earlier stages (F0–2) (Fig. 3B).

Within our cohort, NAS ranged from 0 (mild MASLD) to 7 (most severe MASLD). Notably, six complement genes that underwent hypermethylation in MASLD had relatively high NAS values, whereas three genes that underwent hypomethylation had lower values (Fig. 3C).

To distinguish between MASH and non-MASH, the methylation patterns of the nine complement genes were analyzed according to the SAF score classification. Correlation analysis of the methylation patterns of the nine genes with SAF score revealed more pronounced differences between groups than what was observed for correlation with NAS (Fig. 3D).

To confirm the methylation status of the selected genes

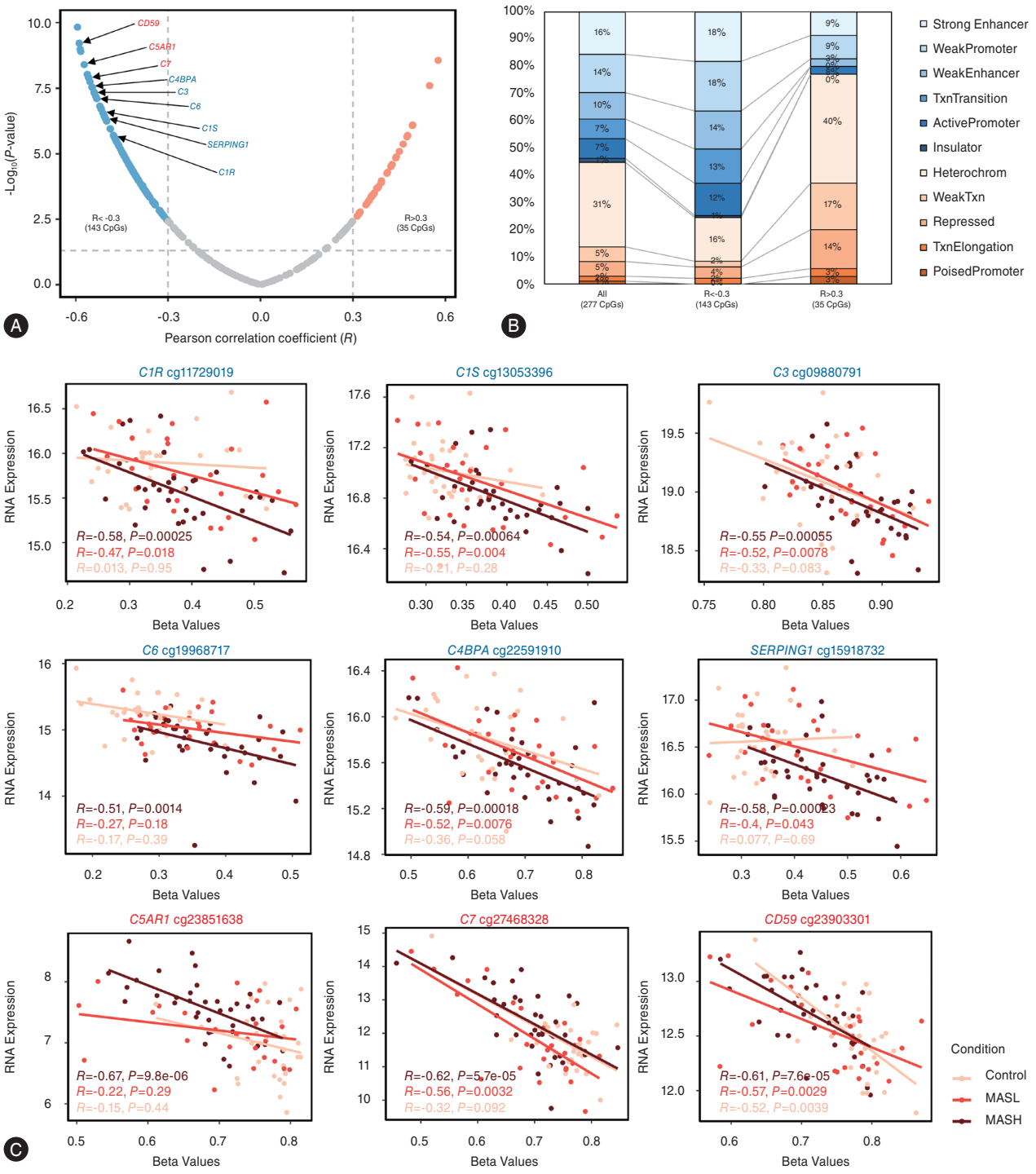

Figure 2. Relationship between DNA methylation and expression of complement genes. (A) Volcano plot depicting Pearson correlations between β values and gene expression values. Negative logarithm (base 10) of *P*-values plotted against Pearson correlations for complement genes. The horizontal dashed line indicates the significance threshold of adjusted *P*-value <0.05, and the vertical dashed lines denote the limits of −0.3 and 0.3 of the Pearson correlation coefficients. (B) Chromatin states and DNA methylation: Distribution of methylation in ChromHMM state elements,[26] with each color representing a distinct ChromHMM state of the genome. The percentage of each ChromHMM state is shown for all CpG sites (left), inversely correlated CpGs (middle), and positively correlated CpGs (right). (C) Correlation between methylation β value and mRNAs transcribed from complement genes. Expression correlated inversely with DNA methylation. The *y* axis represents $\log_2$ transformed gene expression values and the *x* axis represents average β values.

https://doi.org/10.3350/cmh.2024.0229

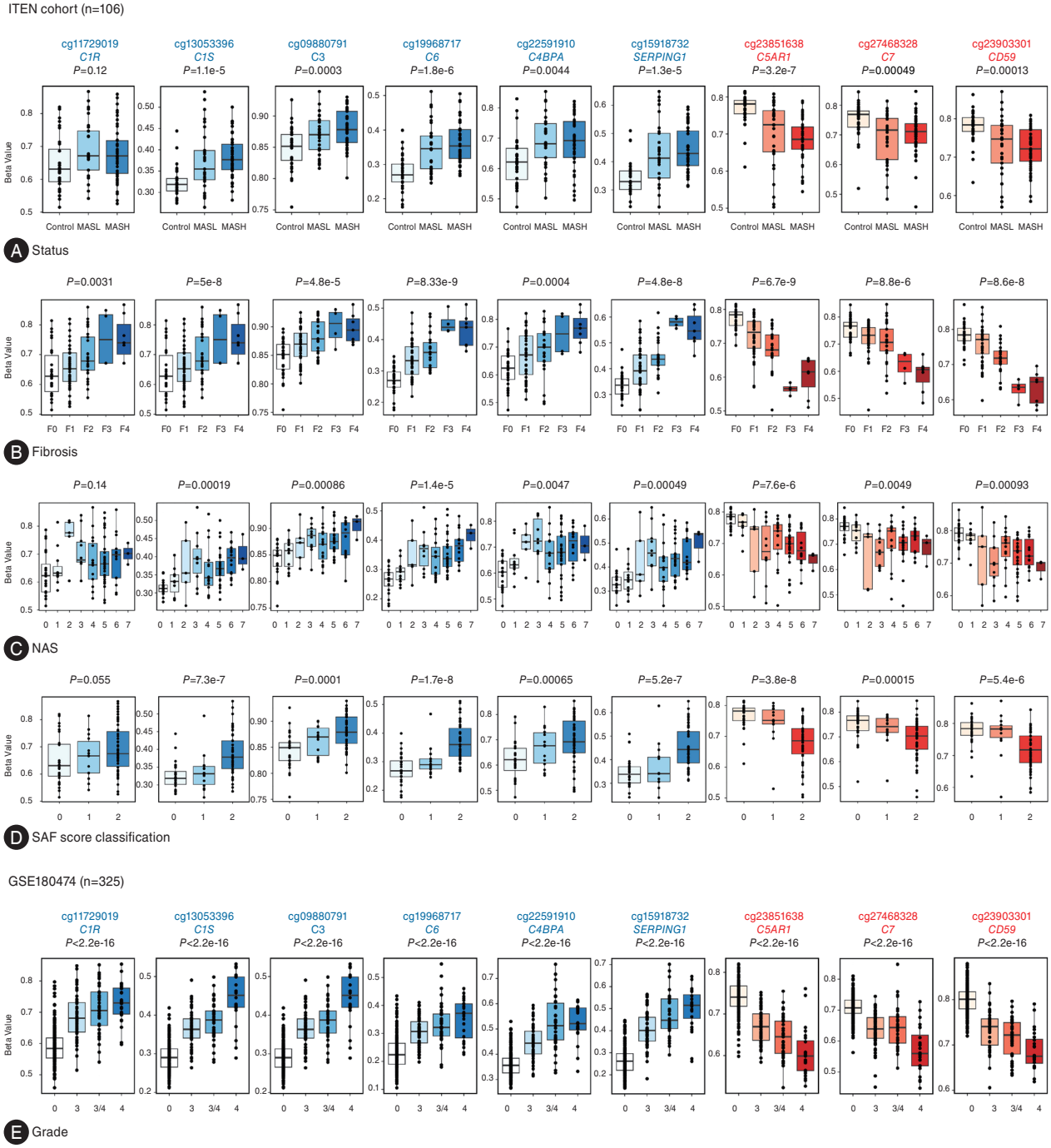

Figure 3. Methylation patterns of nine selected complement genes and correlations with the histological severity spectrum of MASLD. Boxplots illustrating highly differentially methylated complement-related CpG sites in MASLD stages using ITEN cohort data. (A) MASLD groups: Control (n=31), MASL (n=17), and MASH (n=58); (B) fibrotic stage: F0 (n=30), F1 (n=37), F2 (n=26), F3 (n=3), and F4 (n=10); (C) NAFLD activity score (NAS): 0 (n=20), 1 (n=11), 2 (n=5), 3 (n=9), 4 (n=15), 5 (n=31), 6 (n=12), and 7 (n=3); (D) SAF (steatosis, activity and fibrosis) score: 0 (n=31), 1 (n=15), and 2 (n=60). (E) Boxplots for the same CpG sites in the fibrotic stage based on public data (GSE180474).[4] *P*-values indicate the significance of differences among groups (Kruskal–Wallis test). MASLD, metabolic dysfunction-associated steatotic liver disease; MASL, metabolic dysfunction-associated steatotic liver; MASH, metabolic dysfunction–associated steatohepatitis; NAFLD, nonalcoholic fatty liver disease.

in a separate cohort, we utilized publicly available data from GSE180474, which comprises 325 individuals of European ancestry. Among them, 68% had no fibrosis (grade 0), 17% had bridging fibrosis (grade 3), 11% had incomplete cirrhosis (grade 3/4), and 9% had cirrhosis (grade 4). Similar to the findings for our Korean cohort, six complement genes were hypermethylated and the remaining three were hypomethylated, in accordance with fibrosis severity (Fig. 3E), suggesting that these alterations in complement gene methylation were consistent across diverse ethnic groups.

Alterations in complement gene expression during the progression of liver fibrosis

We next investigated the expression patterns of the six hypermethylated and three hypomethylated complement genes in MASLD. Among them, *C1R*, *C1S*, *C3*, *C4BPA*, and *SERPING1* exhibited significantly decreased expression in MASH. Additionally, *C6* was significantly downregulated in MASL, with even further downregulation observed in MASH. In contrast, *C5AR1*, *C7*, and *CD59* were upregulated in MASH (Fig. 4A). Furthermore, the expression of these nine genes in MASLD mirrored the trends observed for liver steatosis (Supplementary Fig. 6), lobular inflammation (Supplementary Fig. 7), and ballooning (Supplementary Fig. 8).

We next analyzed complement gene expression in relation to fibrosis, observing a decrease in the expression of six genes, whereas the remaining three demonstrated increased expression correlating with liver fibrosis (Fig. 4B). Regarding NAS, although *C3* expression did not change significantly, *C1R*, *C1S*, *C6*, *C4BPA*, and *SERPING1* displayed a declining trend in NAS 5 and 6. Conversely, *C5AR1*, *C7*, and *CD59* demonstrated an increasing trend in mRNA levels in cases with severe disease (NAS 5–7) compared with less severe disease (NAS 0–4) (Fig. 4C). Expression of the nine genes differed significantly depending on SAF score (Fig. 4D).

To confirm the expression levels of the nine complement genes in a separate cohort, we utilized publicly available data from GSE135251, which includes 403 European Caucasian patients (381 MASLD samples and 22 control samples).[20] In this dataset, *C1R*, *C1S*, and *SERPING1* exhibited decreased expression, whereas *C5AR1*, *C7*, and *CD59* demonstrated increased expression with respect to the progression of liver fibrosis (Fig. 4E).

As an additional validation of complement gene expression based on fibrosis stage, we utilized SteatoSITE (https://shiny.igc.ed.ac.uk/SteatoSITE_gene_explorer/), which is an open resource comprising data for 940 histologically defined patients spanning the entire spectrum of MASLD severity.[27] Consistent with observations for the Korean ITEN cohort, the six hypermethylated complement genes exhibited reduced expression, whereas the three hypomethylated genes exhibited increased expression, in line with fibrosis severity (Fig. 4F).

To analyze the effect of various factors (antidiabetics, antihypertensive drugs, statins, obesity, and smoking) on the expression of complement genes and DNA methylation patterns, multiple linear regression analysis was conducted. Among the independent variables, DNA methylation was found to have the most significant impact on the expression of complement genes. Specifically, methylation of *C1S*, *C3*, *C6*, *SERPING1*, *C5AR1*, *C7*, and *CD59* was most significantly influenced by MASH status. In contrast, the methylation of *C1R* and *C4BPA* was more significantly affected by antidiabetics than by MASH status. The results of the multiple linear regression analysis indicated that methylation of complement genes is predominantly influenced by MASH status, whereas gene expression is primarily affected by methylation status (Supplementary Table 3).

Altogether, it appears that changes in complement gene expression may influence the progression of liver fibrosis in individuals with MASLD, potentially serving as indicators of the severity and progression of MASLD.

Single-cell analysis of complement gene expression

The liver is composed of various cellular constituents, such as hepatocytes and non-parenchymal cells. To investigate the expression of complement genes across different liver cell types, we analyzed snRNA-seq datasets from the GEO dataset GSE202379.[21] This dataset includes liver biopsies from 47 individuals at different stages of MASLD progression: healthy controls (n=4), MASL (n=7), MASH (n=27), cirrhosis (n=4), and end-stage disease requiring transplantation (n=5).[21] From this analysis, we obtained 99,809 high-quality nuclei, with a significant proportion being hepatocytes (n=69,426).[21] The cell type-specific ex-

https://doi.org/10.3350/cmh.2024.0229

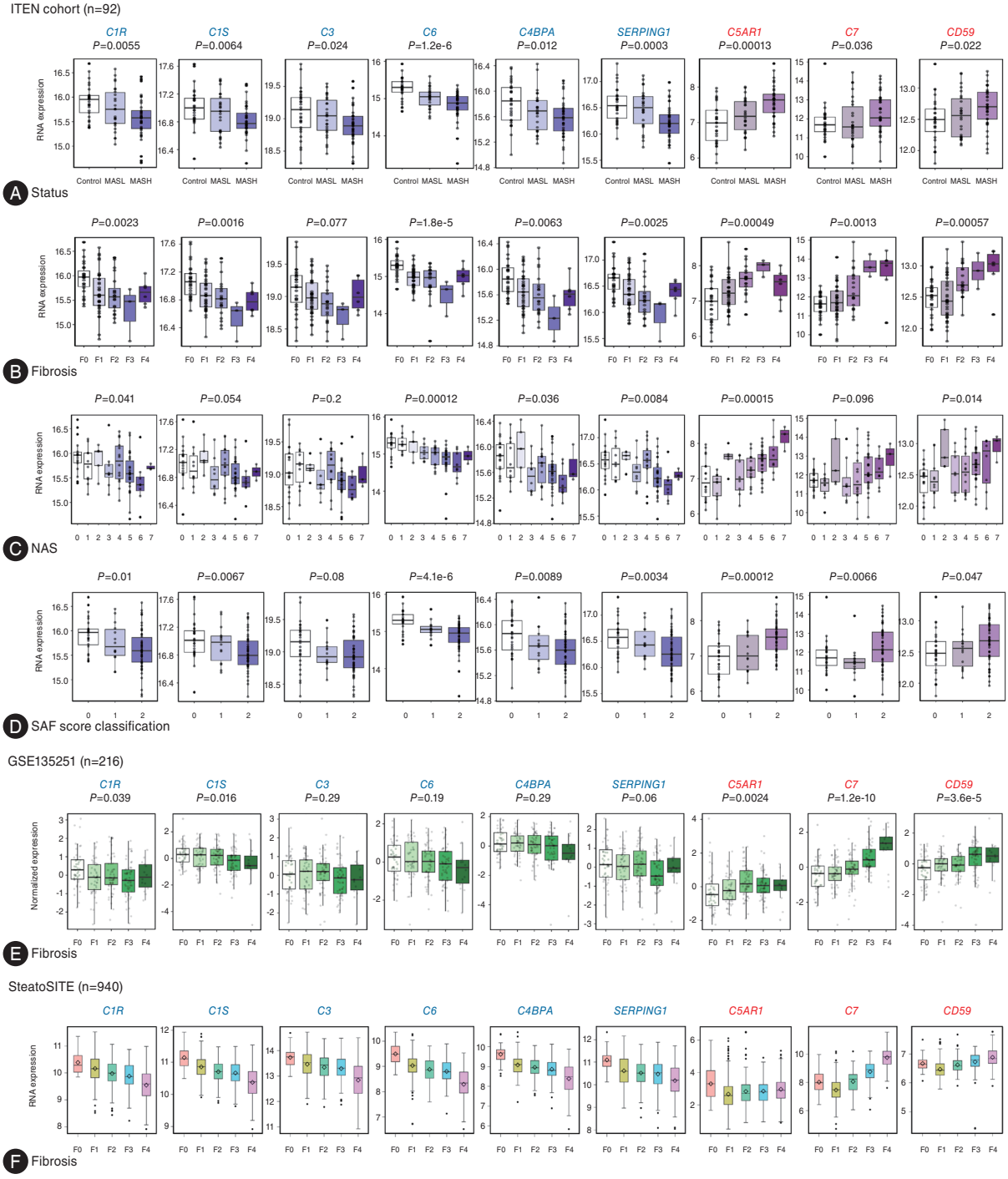

Figure 4. Gene expression patterns of the six hypermethylated and three hypomethylated genes in MASLD. Boxplots for mRNAs expressed according to MASLD stages using ITEN cohort data. (A) MASLD groups: Control (n=28), MASL (n=16), and MASH (n=48); (B) fibrotic stage: F0 (n=27), F1 (n=36), F2 (n=20), F3 (n=3), and F4 (n=6); (C) NAS: 0 (n=18), 1 (n=10), 2 (n=5), 3 (n=8), 4 (n=14), 5 (n=26), 6 (n=8), and 7 (n=3); (D) SAF score: 0 (n=28), 1 (n=14), and 2 (n=50). (E) Boxplots for mRNAs expressed during the fibrotic stage: F0 (n=46), F1 (n=48), F2 (n=54), F3 (n=54), and F4 (n=14) based on public data (GSE135251).[20] *P*-values indicate the significance of differences among groups (Kruskal–Wallis test). (F) Expression of complement genes based on SteatoSITE (https://shiny.igc.ed.ac.uk/SteatoSITE_gene_explorer/), an open resource comprising data for 940 histologically defined MASLD patients.[27] MASLD, metabolic dysfunction-associated steatotic liver disease; MASL, metabolic dysfunction-associated steatotic liver; MASH, metabolic dysfunction–associated steatohepatitis; NAS, NAFLD activity score.

pression levels of complement genes are detailed in Supplementary Figure 9A. Notably, the six hypermethylated genes were predominantly expressed in hepatocytes (Fig. 5A), whereas the three hypomethylated genes (*C7*, *C5AR1*, and *CD59*) exhibited low expression levels (Fig. 5A).

The expression of complement genes throughout disease progression at the single-cell level is illustrated in Supplementary Figure 9B. Notably, the highest expression of complement genes was observed in hepatocyte populations, prompting a focused differential expression analysis on these cells. Across all disease stages, the six complement genes exhibited differential expression, with a marked downregulation observed in end-stage disease, suggesting a correlation between disease progression and the expression of these genes (Fig. 5B). Specifically, in hepatocytes at end-stage disease, there was significant downregulation of *C1R* (logFC=–1.2, FDR=0), *C3* (logFC=–0.97, FDR=0), *C1S* (logFC=–0.4, FDR=3.98×10^{-100}), *SERPING1* (logFC=–0.34, FDR=3.33×10^{-68}), and *C4BPA* (logFC=–0.25, FDR=3.64×10^{-38}) (Fig. 5B). These patterns of downregulation were consistent across other pathological features, including lobular inflammation (Fig. 5C), ballooning (Fig. 5D), and fibrosis (Fig. 5E), underscoring their broader relevance in hepatic pathology.

Hepatocytes arranged along the lobule axis have a zonation pattern marked by spatial disparities in gene expression and metabolic functions.[28,29] Consequently, we investigated complement gene expression in the context of liver zonation. Hepatocyte subpopulations could be classified as periportal (marked by *SDS, HAL, PCK1,* and *ASS1*) and pericentral (*CYP2E1, SLCO1B3,* and *GLUL*) (Fig. 5F). We examined whether complement genes exhibited zonation patterns of expression similar to hepatocytes in healthy tissues (Supplementary Fig. 9C). We found distinct zonation patterns in healthy liver tissue, with similar expression levels of complement genes in periportal and pericentral populations. However, in MASLD, these patterns differed substantially, particularly with regard to downregulation of the six complement genes in central-zone hepatocytes (Supplementary Fig. 9D). This suggests that these genes are predominantly downregulated in cells displaying a central-zone expression pattern in hepatocytes in MASLD tissue. Specifically, *C6* (logFC=–0.7, FDR=1.32×10^{-108}), *C4BPA* (logFC=–0.36, FDR=6.99×10^{-54}), *SERPING1* (logFC=–0.34, FDR=1.84×10^{-37}), and *C3* (logFC=–0.12, FDR=1.18×10^{-41}) were significantly downregulated in central-zone hepatocytes at the end-stage condition (Fig. 5G). Figure 5H and Supplementary Figure 10 illustrate the correlation between the levels of the six complement genes and liver zonation markers. With disease progression, this correlation decreased. These findings suggest a complex relationship between complement gene expression and liver zonation, highlighting the dynamic nature of liver pathology in MASLD.

Expression and methylation of complement genes in a mouse model of MASH

To further investigate DNA methylation and relative expression of the nine complement genes in MASH samples, we conducted a comparative analysis between mice fed a normal diet (n=5) and those fed a MASH diet (n=7). Methylation levels were determined using pyrosequencing, and mRNA levels were measured using RT-qPCR (Fig. 6). The CpG sites analyzed were selected based on their similarity to those studied in humans. Consistent with findings from human samples, the results from the MASH-diet mice validated the involvement of these nine complement genes in pathology. Notably, the methylation levels of *C1ra*, *C3*, *C6*, *C4bpa*, and *Serping1* were significantly elevated in the MASH group, with *C1s1* showing a non-significant increase. Conversely, methylation of *C5ar1* was significantly decreased, whereas no significant differences were observed for *C7* and *Cd59* (Fig. 6B). Additionally, expression of *C1ra*, *C1s1*, *C3*, *C4bpa*, and *Serping1* was significantly reduced in the MASH group, with *C6* showing a non-significant decrease. In contrast, *C5ar1* expression was significantly increased, with *C7* and *Cd59* showing non-significant increases (Fig. 6C). These findings in the MASH mouse model aligned with the human data, further confirming the involvement of these nine genes in MASLD. Specifically, *C1ra*, *C3*, *C4bpa*, and *Serping1* displayed significant hypermethylation and downregulation, whereas *C5ar1* displayed significant hypomethylation and upregulation (Fig. 6).

To elucidate the functional consequences of these epigenetic changes in MASLD pathogenesis, an *in vitro* assay was performed. Mouse hepatocyte cell line AML12 was treated with 200 μM palmitate and 0.5 μg/mL lipopolysaccharide for 12 hours to induce lipogenesis and inflamma-

https://doi.org/10.3350/cmh.2024.0229

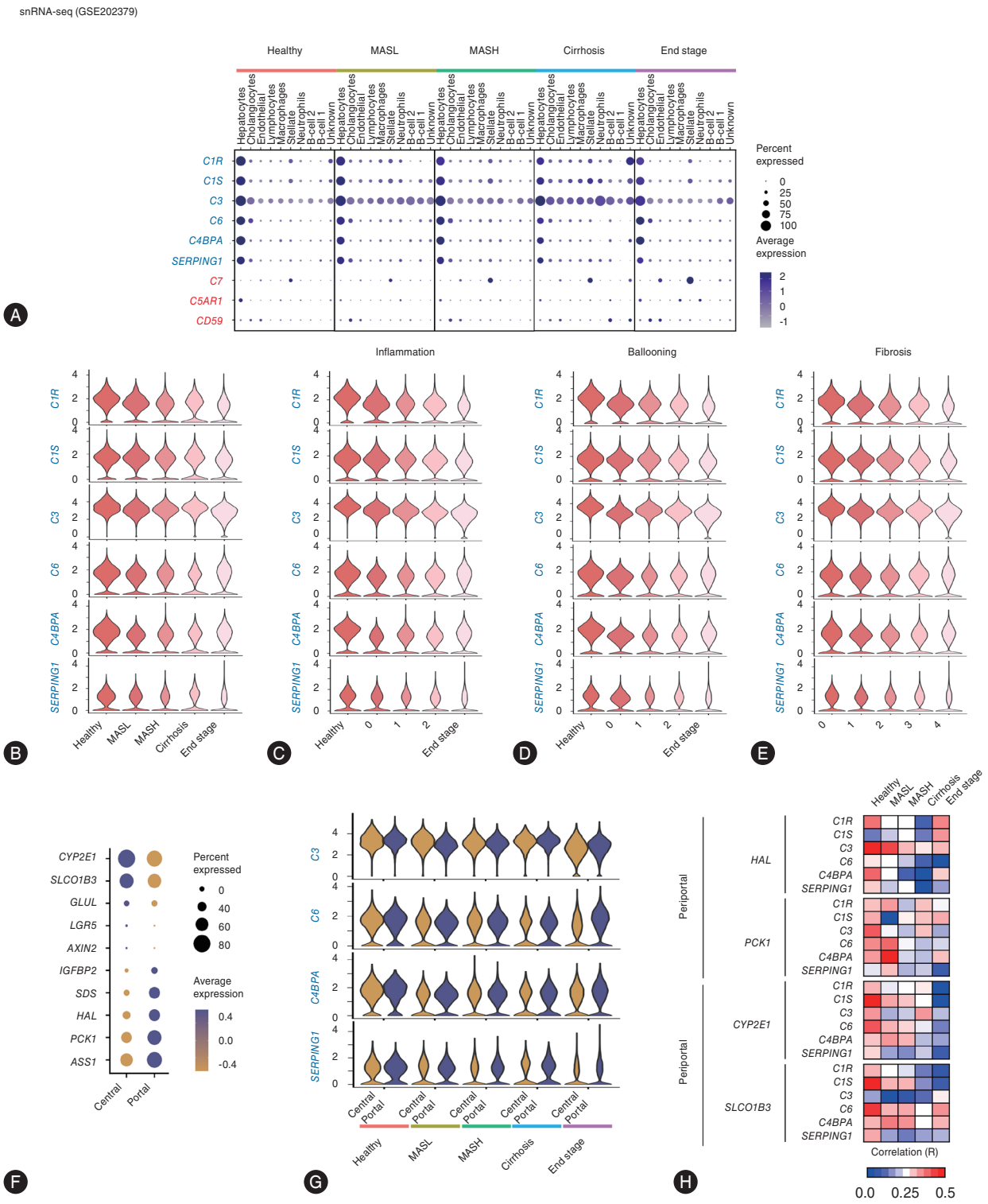

Figure 5. Single-cell expression analysis of complement genes based on public data (GSE202379).[21] (A) Dot plot showing expression of nine genes in each cell type. Circle size represents detection frequency, and color indicates expression level. (B–E) Violin plots showing expression scores for six complement genes in relation to four liver pathologies (B), lobular inflammation (C), ballooning (D), and fibrosis (E). (F) Dot plot showing the average expression of zonation-biased genes in each identified zone. Circle size denotes detection frequency, and color indicates expression level. (G) Violin plots showing expression scores for four complement genes. (H) Correlation between the levels of the six complement genes and liver zonation markers with disease progression.

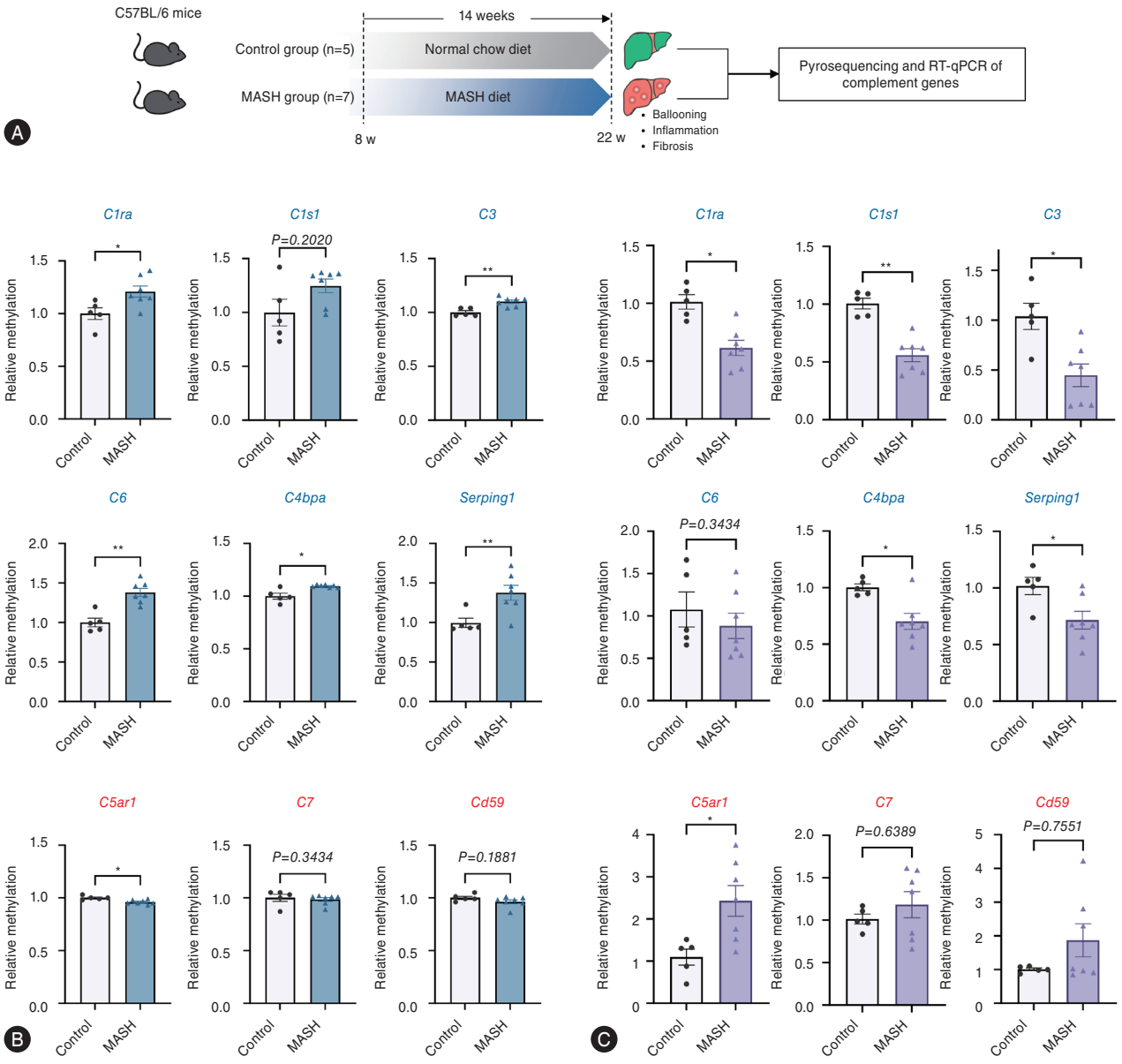

Figure 6. Methylation and expression patterns of nine complement genes in MASH mouse model. (A) Overall scheme for experimental MASH diet mouse model. Experimental MASH was induced in C57BL/6 male mice using a high-fat, high-sucrose diet for 14 weeks. (B) Pyrosequencing and (C) RT-qPCR were performed on nine complement genes in the control group (n=5) and MASH group (n=7). *P*-values indicate the significance of differences between control and MASH mice using the Mann–Whitney U test. ***P*<0.01; **P*<0.05. MASH, metabolic dysfunction–associated steatohepatitis.

tion, followed by treatment with 10 μM AZA, a DNA methylation inhibitor,[30] for 36 hours (Supplementary Fig. 11A). Induction of lipogenesis and inflammation in AML12 cells resulted in decreased expression of *C1s1*, *C3*, *C6*, and *Serping1*, whereas expression of *C5ar1* and *Cd59a* increased (Supplementary Fig. 11B). AZA treatment restored the expression of these complement genes to control levels (Supplementary Fig. 11B). Furthermore, MASLD progression–related genes involved in lipogenesis (*Fasn*, *Scd1*, and *Cd36*), inflammation (*Il6* and *Il1b*), and fibrosis (*Col1a1*) were also restored (Supplementary Fig. 11C). These findings suggested that epigenetic alterations of these complement genes may contribute to MASLD progression and represent potential targets for drug development.

https://doi.org/10.3350/cmh.2024.0229

DISCUSSION

In our research, we provide compelling evidence of epigenetic alteration of complement genes linked to MASLD progression. An integrative analysis of DNA methylome and transcriptome data obtained from liver biopsies of Korean patients with MASLD revealed a consistent pattern: hypermethylation and downregulation of six genes, namely *C1R*, *C1S*, *C3*, *C6*, *C4BPA*, and *SERPING1*, alongside hypomethylation and upregulation of three genes, *C5AR1*, *C7*, and *CD59*. Although similar patterns of DNA methylation and mRNA abundance were observed in European ancestry groups, our study exclusively focused on subjects of East Asian ethnicity. Furthermore, through the integration of publicly accessible datasets, we established a correlation between complement gene expression and liver zonation, elucidating the complex interplay between complement regulation and hepatic pathophysiology. Our findings represent a significant advancement in understanding the functional implications of epigenetic modifications of complement genes in MASLD.

Activation of the complement system involves three proteolytic cascades called the classical, lectin, and alternative pathways, all converging at the activation of C3 convertase, a central point in complement activation. This cascade leads to the activation of crucial effectors such as the membrane attack complex and anaphylatoxins (C3a and C5a), as illustrated in Figure 1A. In the classical pathway, C1q recognizes immune complexes, initiating a chain reaction involving serine proteases C1r and C1s, leading to the activation of C4 and C2. The classical and lectin pathways are activated through binding to complement-fixing antibodies in immune complexes or mannose residues on microorganisms, respectively. In contrast, the alternative pathway undergoes spontaneous activation via continual low-rate hydrolysis of the thioester bond of C3. The resulting activated C3 then binds to factor B, promoting its cleavage into Ba and Bb by factor D. The resulting C3 convertase initiates an amplification loop, generating more C3b and C3a.

Extensive research has increasingly revealed the significant role of the complement system not only in the immune system but also in lipid metabolism. Dysregulated complement activity has been associated with metabolic syndrome, obesity, insulin resistance, and diabetes, all contributing to the development of MASLD.[14,31]

Hepatocytes, which are highly metabolic cells, are also the primary source of extracellular complement synthesis.[32] The six complement genes we identified in the present study (*C1R*, *C1S*, *C3*, *C6*, *C4BPA*, and *SERPING1*), which are primarily expressed in hepatocytes, exhibited elevated methylation in MASLD. Once synthesized and activated, factors encoded by these complement genes may play a vital role in maintaining the normal function and regenerative capacity of hepatocytes.[33,34]

Interestingly, we noted increased methylation and reduced expression of *C3* in liver samples from MASLD patients, which contradicts previous findings of elevated levels of C3 in plasma of MASLD patients.[35] Moreover, type 2 diabetes is linked to heightened systemic concentrations of C3.[36] Given the frequent concurrence of MASLD and type 2 diabetes, it is plausible that the observed heightened C3 levels could originate from sources beyond the liver, such as adipose tissue.[37,38]

Our observations of reduced *C3* expression in the MASH group are supported by the findings of Segers et al., who reported significantly diminished liver *C3* mRNA and protein levels in individuals with MASH.[39] Specifically, in mouse hepatocytes, it has been elucidated that C3 has a protective role against hepatic steatosis by influencing lipophagy, a specialized form of autophagy targeting lipid droplets in liver triglyceride breakdown.[40] Additionally, intracellular C3 has been shown to promote the assembly and secretion of very low–density lipoprotein, thereby assisting in the reduction of lipid accumulation within hepatocytes.[40] These insights underscore the multifaceted roles of C3 in lipid metabolism in the liver with potential implications in metabolic liver diseases.

Besides parenchymal cells, the liver houses various nonparenchymal and immune cells like macrophages, stellate cells, and lymphoid cells. Consequently, the liver is not only a metabolic center but also an immune organ responsible for maintaining whole-body homeostasis under normal conditions. The three complement genes (*C7*, *C5AR1*, and *CD59*) that we found were primarily expressed in non-parenchymal cells were hypomethylated and upregulated in MASLD specimens. Epigenetic alterations of these genes could result in abnormalities in the innate immune response, potentially culminating in liver injury and fibrosis.[41,42] As pivotal components of the innate immune re-

sponse, aberrant activation of these genes might contribute to the progression of MASLD by impacting various immune cell populations within the liver.[10]

It has been established that the C5a/C5aR pathway is involved in promoting macrophage accumulation and M1-like polarization within white adipose tissue of obese mice, leading to insulin resistance.[43] This suggests that heightened expression of C5aR may contribute to the development of MASLD by activating Kupffer cells/macrophages. Notably, Castellano et al.[44] observed that exposure to C5a resulted in widespread hypomethylation across the genome of human renal tubular epithelial cells, specifically affecting genes involved in cell cycle regulation, DNA damage response, and Wnt signaling pathways.[44] indicating that epigenetic changes of complement genes could both instigate and result from altered complement gene expression in MASLD.

C7 is a terminal component of the complement cascade. Elevated concentrations of C7 in plasma have been linked to MASH with advanced fibrosis.[45,46] In a study by Wei Hou et al.[46], high levels of Complement C7 were associated with advanced fibrosis in MASH patients and effectively classified these patients in a pilot study.[45,46] This study also found that C7, along with other complement proteins, significantly correlated with liver stiffness, suggesting its potential as a biomarker for advanced fibrosis in MAFLD.[45,46] Consistent with other proteomic investigations, our study observed reduced methylation of *C7* and elevated levels of its mRNA in the liver tissue of MASH patients with advanced fibrosis. These findings suggest a potentially significant role of C7 in MASLD pathogenesis. However, further research is needed to elucidate the precise mechanisms by which C7 influences the progression of MASLD.

CD59 is a membrane complement regulatory protein that plays a crucial role in preventing the formation of the membrane attack complex and maintaining control over complement activation. CD59 is found abundantly across diverse cell types in vertebrates, encompassing blood cells, endothelial cells, and epithelial cells.[47] Diminished methylation of *CD59* and elevated levels of its mRNA might lead to an imbalance in complement activation and inhibition, thereby impacting the progression of MASLD. Additional investigation is needed for a deeper understanding of these mechanisms.

Hepatic zonation, a fundamental feature of liver structure, denotes the partitioning of liver lobules into specialized functional regions along the porto-central axis. Each of these regions has distinct metabolic and physiological traits, facilitating specialized functions and interactions within the liver.[29] Periportal hepatocytes oversee energy-intensive tasks like xenobiotic metabolism, bile acid synthesis, and glycolysis. Conversely, central hepatocytes are responsible for less demanding functions such as β-oxidation, cholesterol biosynthesis, protein secretion, and gluconeogenesis.[29] The initial progression of MASLD primarily takes place in the pericentral region, with steatosis extending along the porto-central axis.[48] In hepatocytes from MASLD tissue, we noted a reduction in complement gene expression predominantly in cells showing a central-zone expression pattern. Further research is required to deepen our understanding of the complex interaction between these spatial factors and the trajectory of MASLD.

Blocking the complement system has emerged as a promising approach to hinder the progression of MASH, potentially opening avenues for innovative treatment modalities.[10] Presently, more than 20 therapeutic agents are in clinical development, each aimed at distinct components and pathways within the complement cascade, addressing various indications.[49] The complement cascade offers numerous opportunities for therapeutic intervention, each with its own set of advantages and disadvantages depending on the clinical context and underlying pathophysiology. However, inappropriate or nonspecific modulation of the complement system carries a significant risk of adverse effects, such as increased susceptibility to infections.[9]

Our findings indicate that targeting C5/C5aR holds promise for anti-MASH therapy. Drugs, such as eculizumab, ravulizumab, and avacopan, which target C5/C5aR, have already been approved for clinical use to treat conditions such as atypical hemolytic uremic syndrome or anti-neutrophil cytoplasmic antibody–associated vasculitis.[50,51] Encouragingly, preclinical studies utilizing antagonists against C5aR have demonstrated protective effects against diet-induced obesity and metabolic dysfunction.[52] However, further investigation is warranted for the clinical application of targeting C5/C5aR for MASH treatment.

This study's limitations include the lack of experimental validation regarding the therapeutic aspects of targeting the complement system for MASH, which should be conducted in future research. Moreover, any cross-sectional

https://doi.org/10.3350/cmh.2024.0229

study aiming to elucidate changes in both DNA methylation and gene expression in MASLD faces inherent constraints. Enhancing the evidence base through secondary data analysis from longitudinal studies or interventional trials would better delineate causality and temporal relationships between variables.

Furthermore, this study categorized biopsy specimens into the control and MASLD groups based on standardized histological scores. There are potential limitations, however, in that sample selection may have inherent biases, and the criteria for categorization could introduce confounding factors that affect the observed methylation and expression patterns of complement genes. Additionally, the sample size in this study was relatively small compared to other open-source studies, and we relied on snRNA-seq data from a public database representing a different ethnic population rather than utilizing our own data. To address this, it is essential to validate these findings in a larger sample group.

Although our dataset included information on lifestyle factors, comorbidities, and related medications, it sometimes contained only non-quantitative data for some samples. These limitations hindered any comprehensive analysis of all variables in this study, indicating that further research is needed to identify additional factors that influence DNA methylation patterns and gene expression levels in liver samples from MASLD patients. Moreover, the study did not collect liver tissue samples from an independent patient group, thus preventing the isolation and analysis of genomic DNA from liver tissue. To address these limitations, future research should aim to validate our findings in an independent MASLD cohort, ensuring a more robust understanding of epigenetic mechanisms involved in MASLD.

In summary, our study reveals, for the first time, the epigenetic and transcriptional changes in complement genes in the liver during the progression of MASLD. These findings have potential implications for understanding the core mechanisms underlying MASLD progression and for developing targeted therapeutic approaches.

Authors' contribution

M.K. and W.K. conceived and designed the study. D.H.L., and W.K. contributed to sample acquisition. H.-J.K., J.M.L., H.A.S., K.H., and H.-J.J. contributed to sample processing, quality control and data generation. A.M., H.-J.K., H.G., H.J., E.-S.K., T.Y., M.C., K.W.K., W.K., and M.K. contributed to data analysis and interpretation. A.M., H.-J.K., W.K., and M.K. wrote the manuscript with contributions from all authors. M.K. and W.K. supervised the research and are the guarantors of this work. All authors read and approved the final manuscript.

Acknowledgements

This work was supported by a National Research Foundation of Korea (NRF) grant funded by the Korean government (RS-2024-00440883, 2023R1A2C1003339, 2021R1A2C2005820, 2022M3A9B6017654, RS-2023-00223831, and 2021M3A9E4021818), the Korea Health Technology R&D Project through the Korea Health Industry Development Institute (KHIDI) funded by the Ministry of Health & Welfare, Republic of Korea (HI21C0538), National Research Council of Science & Technology (NST) Aging Convergence Research Center (CRC22013-400), a Korea National Institute of Health (KNIH) research project (2022ER090202), the Korea Research Institute of Bioscience & Biotechnology (KRIBB) Research Initiative Program (KGM5192423), and a multidisciplinary research grant-in-aid from the Seoul Metropolitan Government Seoul National University (SMG-SNU) Boramae Medical Center (04-2023-0032, 04-2023-0033).

Conflicts of Interest

The authors declare no competing interests.

SUPPLEMENTARY MATERIAL

Supplementary material is available at Clinical and Molecular Hepatology website (http://www.e-cmh.org).

The data that support the findings of this study are available from the corresponding authors, upon reasonable request. The raw data for this study were deposited in K-BDS (Korea BioData Station, https://kbds.re.kr) under accession number KAP240571.

REFERENCES

1. Rinella ME, Lazarus JV, Ratziu V, Francque SM, Sanyal AJ,

Kanwal F, et al. A multisociety Delphi consensus statement on new fatty liver disease nomenclature. J Hepatol 2023;79:1542-1556.
2. Le MH, Yeo YH, Zou B, Barnet S, Henry L, Cheung R, et al. Forecasted 2040 global prevalence of nonalcoholic fatty liver disease using hierarchical bayesian approach. Clin Mol Hepatol 2022;28:841-850.
3. Lim HJ, Kim M. EZH2 as a potential target for NAFLD therapy. Int J Mol Sci 2020;21:8617.
4. Johnson ND, Wu X, Still CD, Chu X, Petrick AT, Gerhard GS, et al. Differential DNA methylation and changing cell-type proportions as fibrotic stage progresses in NAFLD. Clin Epigenetics 2021;13:152.
5. Murphy SK, Yang H, Moylan CA, Pang H, Dellinger A, Abdelmalek MF, et al. Relationship between methylome and transcriptome in patients with nonalcoholic fatty liver disease. Gastroenterology 2013;145:1076-1087.
6. Ricklin D, Hajishengallis G, Yang K, Lambris JD. Complement: a key system for immune surveillance and homeostasis. Nat Immunol 2010;11:785-797.
7. Schraufstatter IU, Khaldoyanidi SK, DiScipio RG. Complement activation in the context of stem cells and tissue repair. World J Stem Cells 2015;7:1090-1108.
8. Zhou Y, Yuan G, Zhong F, He S. Roles of the complement system in alcohol-induced liver disease. Clin Mol Hepatol 2020;26:677-685.
9. Ricklin D, Reis ES, Lambris JD. Complement in disease: a defence system turning offensive. Nat Rev Nephrol 2016;12:383-401.
10. Guo Z, Fan X, Yao J, Tomlinson S, Yuan G, He S. The role of complement in nonalcoholic fatty liver disease. Front Immunol 2022;13:1017467.
11. Zhao J, Wu Y, Lu P, Wu X, Han J, Shi Y, et al. Association of complement components with the risk and severity of NAFLD: a systematic review and meta-analysis. Front Immunol 2022;13:1054159.
12. Lung T, Sakem B, Risch L, Würzner R, Colucci G, Cerny A, et al. The complement system in liver diseases: evidence-based approach and therapeutic options. J Transl Autoimmun 2019;2:100017.
13. Bavia L, Cogliati B, Dettoni JB, Ferreira Alves VA, Isaac L. The complement component C5 promotes liver steatosis and inflammation in murine non-alcoholic liver disease model. Immunol Lett 2016;177:53-61.
14. Nguyen VD, Hughes TR, Zhou Y. From complement to complosome in non-alcoholic fatty liver disease: when location matters. Liver Int 2024;44:316-329.
15. Han J, Zhang X. Complement component C3: a novel biomarker participating in the pathogenesis of non-alcoholic fatty liver disease. Front Med (Lausanne) 2021;8:653293.
16. Yoo T, Joo SK, Kim HJ, Kim HY, Sim H, Lee J, et al. Disease-specific eQTL screening reveals an anti-fibrotic effect of AGXT2 in non-alcoholic fatty liver disease. J Hepatol 2021;75:514-523.
17. Koo BK, Joo SK, Kim D, Bae JM, Park JH, Kim JH, et al. Additive effects of PNPLA3 and TM6SF2 on the histological severity of non-alcoholic fatty liver disease. J Gastroenterol Hepatol 2018;33:1277-1285.
18. Brunt EM, Kleiner DE, Wilson LA, Belt P, Neuschwander-Tetri BA; NASH Clinical Research Network (CRN). Nonalcoholic fatty liver disease (NAFLD) activity score and the histopathologic diagnosis in NAFLD: distinct clinicopathologic meanings. Hepatology 2011;53:810-820.
19. Bedossa P, Poitou C, Veyrie N, Bouillot JL, Basdevant A, Paradis V, et al. Histopathological algorithm and scoring system for evaluation of liver lesions in morbidly obese patients. Hepatology 2012;56:1751-1759.
20. Govaere O, Cockell S, Tiniakos D, Queen R, Younes R, Vacca M, et al. Transcriptomic profiling across the nonalcoholic fatty liver disease spectrum reveals gene signatures for steatohepatitis and fibrosis. Sci Transl Med 2020;12:eaba4448.
21. Gribben C, Galanakis V, Calderwood A, Williams EC, Chazarra-Gil R, Larraz M, et al. Acquisition of epithelial plasticity in human chronic liver disease. Nature 2024;630:166-173.
22. Halpern KB, Shenhav R, Massalha H, Toth B, Egozi A, Massasa EE, et al. Paired-cell sequencing enables spatial gene expression mapping of liver endothelial cells. Nat Biotechnol 2018;36:962-970.
23. MacParland SA, Liu JC, Ma XZ, Innes BT, Bartczak AM, Gage BK, et al. Single cell RNA sequencing of human liver reveals distinct intrahepatic macrophage populations. Nat Commun 2018;9:4383.
24. Aizarani N, Saviano A, Sagar, Mailly L, Durand S, Herman JS, et al. A human liver cell atlas reveals heterogeneity and epithelial progenitors. Nature 2019;572:199-204.
25. Guilliams M, Bonnardel J, Haest B, Vanderborght B, Wagner C, Remmerie A, et al. Spatial proteogenomics reveals distinct and evolutionarily conserved hepatic macrophage niches. Cell 2022;185:379-396.e38.
26. Roadmap Epigenomics Consortium; Kundaje A, Meuleman

W, Ernst J, Bilenky M, Yen A, et al. Integrative analysis of 111 reference human epigenomes. Nature 2015;518:317-330.
27. Kendall TJ, Jimenez-Ramos M, Turner F, Ramachandran P, Minnier J, McColgan MD, et al. An integrated gene-to-outcome multimodal database for metabolic dysfunction-associated steatotic liver disease. Nat Med 2023;29:2939-2953.
28. Paris J, Henderson NC. Liver zonation, revisited. Hepatology 2022;76:1219-1230.
29. Ben-Moshe S, Shapira Y, Moor AE, Manco R, Veg T, Bahar Halpern K, et al. Spatial sorting enables comprehensive characterization of liver zonation. Nat Metab 2019;1:899-911.
30. Jones PA, Taylor SM. Cellular differentiation, cytidine analogs and DNA methylation. Cell 1980;20:85-93.
31. Shi Y, Dong H, Sun S, Wu X, Fang J, Zhao J, et al. Protein-centric omics analysis reveals circulating complements linked to non-viral liver diseases as potential therapeutic targets. Clin Mol Hepatol 2024;30:80-97.
32. Lubbers R, van Essen MF, van Kooten C, Trouw LA. Production of complement components by cells of the immune system. Clin Exp Immunol 2017;188:183-194.
33. Markiewski MM, Mastellos D, Tudoran R, DeAngelis RA, Strey CW, Franchini S, et al. C3a and C3b activation products of the third component of complement (C3) are critical for normal liver recovery after toxic injury. J Immunol 2004;173:747-754.
34. Mastellos D, Papadimitriou JC, Franchini S, Tsonis PA, Lambris JD. A novel role of complement: mice deficient in the fifth component of complement (C5) exhibit impaired liver regeneration. J Immunol 2001;166:2479-2486.
35. Yesilova Z, Ozata M, Oktenli C, Bagci S, Ozcan A, Sanisoglu SY, et al. Increased acylation stimulating protein concentrations in nonalcoholic fatty liver disease are associated with insulin resistance. Am J Gastroenterol 2005;100:842-849.
36. Engström G, Hedblad B, Eriksson KF, Janzon L, Lindgärde F. Complement C3 is a risk factor for the development of diabetes: a population-based cohort study. Diabetes 2005;54:570-575.
37. Naughton MA, Botto M, Carter MJ, Alexander GJ, Goldman JM, Walport MJ. Extrahepatic secreted complement C3 contributes to circulating C3 levels in humans. J Immunol 1996;156:3051-3056.
38. Wlazlo N, van Greevenbroek MM, Ferreira I, Jansen EJ, Feskens EJ, van der Kallen CJ, et al. Low-grade inflammation and insulin resistance independently explain substantial parts of the association between body fat and serum C3: the CODAM study. Metabolism 2012;61:1787-1796.
39. Segers FM, Verdam FJ, de Jonge C, Boonen B, Driessen A, Shiri-Sverdlov R, et al. Complement alternative pathway activation in human nonalcoholic steatohepatitis. PLoS One 2014;9:e110053.
40. Li Y, Sha Y, Wang H, He L, Li L, Wen S, et al. Intracellular C3 prevents hepatic steatosis by promoting autophagy and very-low-density lipoprotein secretion. FASEB J 2021;35:e22037.
41. Krenkel O, Tacke F. Liver macrophages in tissue homeostasis and disease. Nat Rev Immunol 2017;17:306-321.
42. Robinson MW, Harmon C, O'Farrelly C. Liver immunology and its role in inflammation and homeostasis. Cell Mol Immunol 2016;13:267-276.
43. Phieler J, Chung KJ, Chatzigeorgiou A, Klotzsche-von Ameln A, Garcia-Martin R, Sprott D, et al. The complement anaphylatoxin C5a receptor contributes to obese adipose tissue inflammation and insulin resistance. J Immunol 2013;191:4367-4374.
44. Castellano G, Franzin R, Sallustio F, Stasi A, Banelli B, Romani M, et al. Complement component C5a induces aberrant epigenetic modifications in renal tubular epithelial cells accelerating senescence by Wnt4/βcatenin signaling after ischemia/reperfusion injury. Aging (Albany NY) 2019;11:4382-4406.
45. Bell LN, Theodorakis JL, Vuppalanchi R, Saxena R, Bemis KG, Wang M, et al. Serum proteomics and biomarker discovery across the spectrum of nonalcoholic fatty liver disease. Hepatology 2010;51:111-120.
46. Hou W, Janech MG, Sobolesky PM, Bland AM, Samsuddin S, Alazawi W, et al. Proteomic screening of plasma identifies potential noninvasive biomarkers associated with significant/advanced fibrosis in patients with nonalcoholic fatty liver disease. Biosci Rep 2020;40:BSR20190395.
47. Wang Z, Guo W, Liu Y, Gong Y, Ding X, Shi K, et al. Low expression of complement inhibitory protein CD59 contributes to humoral autoimmunity against astrocytes. Brain Behav Immun 2017;65:173-182.
48. Chalasani N, Wilson L, Kleiner DE, Cummings OW, Brunt EM, Unalp A, et al. Relationship of steatosis grade and zonal location to histological features of steatohepatitis in adult patients with non-alcoholic fatty liver disease. J Hepatol 2008;48:829-834.
49. Mastellos DC, Ricklin D, Lambris JD. Clinical promise of next-generation complement therapeutics. Nat Rev Drug Discov 2019;18:707-729.
50. Jayne DRW, Merkel PA, Bekker P. Avacopan for the treatment of ANCA-associated vasculitis. Reply. N Engl J Med 2021;384:e81.

51. Wijnsma KL, Duineveld C, Wetzels JFM, van de Kar NCAJ. Eculizumab in atypical hemolytic uremic syndrome: strategies toward restrictive use. Pediatr Nephrol 2019;34:2261-2277.
52. Lim J, Iyer A, Suen JY, Seow V, Reid RC, Brown L, et al. C5aR and C3aR antagonists each inhibit diet-induced obesity, metabolic dysfunction, and adipocyte and macrophage signaling. FASEB J 2013;27:822-831.

https://doi.org/10.3350/cmh.2024.0229